



## Characterization of organic nitrogen in aerosols at a forest site in the southern Appalachian Mountains

Xi Chen<sup>1</sup>, Mingjie Xie<sup>2,a</sup>, Michael D. Hays<sup>1</sup>, Eric Edgerton<sup>3</sup>, Donna Schwede<sup>4</sup>, John T. Walker<sup>1,\*</sup>

<sup>1</sup>National Risk Management Research Laboratory, Office of Research and Development, U.S. Environmental Protection Agency, Research Triangle Park, North Carolina, 27711, U.S.A.

<sup>2</sup>Oak Ridge Institute for Science and Education (ORISE), National Risk Management Research Laboratory, Office of Research and Development, U.S. Environmental Protection Agency, Research Triangle Park, North Carolina, 27711, U.S.A.

<sup>3</sup>Atmospheric Research and Analysis, Inc., Cary, NC, 27513

<sup>4</sup>National Exposure Research Laboratory, Office of Research and Development, U.S. Environmental Protection Agency, Research Triangle Park, North Carolina, 27711, U.S.A.

<sup>a</sup>Present address: School of Environmental Science and Engineering, Nanjing University of Information Science & Technology, Nanjing 210044, China

\*Corresponding Author: Tel.: +1 919 541 2288. Email: Walker.JohnT@epa.gov.

### Abstract

This study investigates the composition of organic particulate matter in a remote montane forest in the southeastern U.S., focusing on the role of organic nitrogen (N) in sulfur-containing secondary organic aerosol (nitrooxy-organosulfates) and aerosols associated with biomass burning (nitro-aromatics). Bulk water soluble organic N (WSON) represented ~ 14% w/w of water soluble total N (WSTN) in PM<sub>2.5</sub>, on average, across seasonal measurement campaigns conducted in the spring, summer, and fall of 2015. Largest contributions of WSON to WSTN were observed in spring (~ 18% w/w) and lowest in the fall (~10% w/w). On average, identified nitro-aromatic and nitrooxy-organosulfate compounds accounted for a small fraction of WSON, ranging from ~ 1% in spring to ~ 4% in fall, though were observed to contribute as much as 28% w/w of WSON in individual samples. Highest concentrations of oxidized organic N species occurred during summer (average of 0.65 ngN/m<sup>3</sup>) along with a greater relative abundance of higher generation oxygenated terpenoic acids, indicating an association with more aged aerosol.



Highest concentrations of nitro-aromatics (eg. nitrocatechol and methyl-nitrocatechol), levoglucosan, and aged SOA tracers were observed during fall, associated with aged biomass burning plumes. Nighttime nitrate radical chemistry is the most likely formation pathway for nitrooxy-organosulfates observed at this low NO<sub>x</sub> site (generally <1ppb). Isoprene derived organosulfate (MW216, 2-methyltetrol derived), which is formed from isoprene epoxydiols (IEPOX) under low NO<sub>x</sub> conditions, was the most abundant individual organosulfate. Concentration weighted average N/C ratios for nitro-aromatics + organosulfates + terpenoid acids were one order of magnitude lower than the overall aerosol N/C ratio, indicating the presence of other uncharacterized higher N content species. Although nitrooxy-organosulfates and nitro-aromatics contributed a small fraction of WSON, our results provide new insight into the atmospheric formation processes and sources of these largely uncharacterized components of atmospheric organic N, which also helps to advance the atmospheric models to better understand the chemistry and deposition of reactive N.

49

## 50 1. Introduction

51

There is extensive evidence showing that boreal and temperate forests are affected by anthropogenic activities, both industrial and agricultural. Such activity results in unprecedented quantities of reactive nitrogen (N) being released into the atmosphere, subsequently altering global nitrogen and carbon (C) biogeochemical cycles (Bragazza et al., 2006; Doney et al., 2007; Ollinger et al., 2002; Magnani et al., 2007; Neff et al., 2002a,b; Pregitzer et al., 2008). Nitrogen enters natural ecosystems through atmospheric deposition and biological fixation, and is mainly lost through leaching and gaseous fluxes back to the atmosphere (Hungate et al., 2003). Atmospheric deposition of N to terrestrial ecosystems may lead to soil and aquatic acidification, nutrient imbalance and enrichment, plant damage and microbial community changes as well as loss of biodiversity (Bobbink et al., 1998; Magnani et al., 2007; Lohse et al., 2008; Simkin et al., 2016).

In the United States, deposition of atmospheric pollutants including N is monitored by the National Atmospheric Deposition Program (NADP) and EPA's Clean Air Status and Trends Network (CASNET). However, these networks focus only on inorganic N species (eg. NH<sub>3</sub>/NH<sub>4</sub><sup>+</sup> and HNO<sub>3</sub>/NO<sub>3</sub><sup>-</sup>). Recent studies shed light on the importance of organic N deposition, which is not routinely measured in national networks. On a global basis, organic N



68 may contribute ~ 25 percent of the total N deposition (Gonzalez Benitez et al., 2009; Jickells et  
69 al., 2013; Keene et al., 2002; Neff et al., 2002a; Zhang et al., 2012). Although ubiquitous,  
70 widespread routine monitoring of organic N in the atmosphere is inhibited due to difficulties in  
71 sampling (Walker et al., 2012) and inability to fully speciate the wide range of constituents that  
72 make up this large pool of atmospheric N (Altieri et al., 2009; Cape et al., 2011; Neff et al.,  
73 2002a; Samy et al., 2013). For these reasons, understanding of the sources, atmospheric  
74 chemistry, and deposition of organic nitrogen remains limited.

75       Atmospheric N from biogenic and anthropogenic emissions sources undergoes complex  
76 transformation processes and photochemical reactions. Consequently, apportionment of  
77 atmospheric organic N to potential sources is challenging. However, such information is required  
78 to advance atmospheric N models applied to better understand the global N cycle. For example,  
79 Miyazaki et al. (2014) examined aerosols collected in a deciduous forest and found in the  
80 summer that water soluble organic N (WSO<sub>N</sub>) correlated positively to biogenic hydrocarbon  
81 oxidation; and during fall WSO<sub>N</sub> in the coarse particle fraction was associated with primary  
82 biological emissions (e.g. emitted from soil, vegetation, pollen and bacteria). Such patterns  
83 underscore that atmospheric organic N measured in forested landscapes originates from a variety  
84 of sources that contribute differently across seasons.

85       Recent advancements have been made in speciation of organic N in aerosol for some  
86 groups of compounds including amines, amino acids and other nitrogenated functional groups  
87 such as organonitrates (Day et al., 2010; Place et al., 2017; Samy et al., 2013). Organic N in  
88 secondary aerosol and aerosols associated with biomass burning sources are areas of increasing  
89 interest, from both atmospheric chemistry and ecosystem exposure perspectives, where more  
90 information is needed. Studies of secondary organic aerosols (SOA) have identified a variety of  
91 nitrated organosulfate compounds (e.g. nitrooxy-organosulfates) in both chamber and ambient  
92 aerosol samples following isoprene and monoterpenes oxidation. These compounds are either  
93 produced under high NO<sub>x</sub> conditions or from nighttime NO<sub>3</sub> radical chemistry (Surratt et al.,  
94 2006, 2007, 2008, 2010; Darer et al., 2011; Lin et al., 2013a; He et al., 2014; Worton et al.,  
95 2013). Potential SOA precursors such as unsaturated green leaf volatiles (GLVs) released by  
96 wounded plants (e.g. crop harvesting and insect attacks) may contribute substantially to the  
97 budget of biogenic SOA formation especially in remote forests (Gomez-Gonzalez et al., 2008;  
98 Hamilton et al., 2013; Shalamzari et al., 2016). The detection of reaction products such as



99 organosulfates and nitrooxy-organosulfates in ambient aerosols provides strong evidence of  
100 influence from anthropogenic sources (e.g. SO<sub>2</sub> and NO<sub>x</sub>) interacting with biogenic precursors to  
101 form nitrogenated SOA (Chan et al., 2010; Lin et al., 2013a; Meade et al., 2016).

102 In addition to being present in sulfur-containing SOA, organic nitrogen, specifically  
103 nitro-aromatic compounds (e.g. nitrophenols and nitrocatechols), have been characterized as  
104 chemical tracers from biomass burning (e.g. wildland and prescribed smoke, bushfires,  
105 residential wood burning). This is in addition to levoglucosan, a widely used tracer of biomass  
106 burning (Iinuma et al., 2010, 2016; Kahnt et al., 2013; Kitanovski et al., 2012; Gaston et al.,  
107 2016). These nitrated compounds can form during pyrolysis of plant biopolymers such as  
108 cellulose. Furthermore, as combustion byproducts, these compounds are often defined as brown  
109 carbon (BrC) and thus potentially light absorbing (Mohr et al., 2013; Liu et al., 2015).  
110 Presumably, nitro-aromatics could constitute a substantial portion of atmospheric organic N in  
111 aerosols collected in regions affected by biomass burning.

112 This study investigates the composition of organic particulate matter in a remote montane  
113 forest in the southeastern U.S., focusing on the role of organic N in sulfur-containing SOA and  
114 aerosols associated with biomass burning. Measurements target four groups of compounds: 1)  
115 nitro-aromatics associated with biomass burning; 2) organosulfates and nitrooxy-organosulfates  
116 produced from biogenic SOA precursors (i.e., isoprene, monoterpenes and unsaturated  
117 aldehydes) interacting with anthropogenic pollutants; 3) terpenoic acids formed from  
118 monoterpene oxidation; and 4) organic molecular markers including methyltetrols, C-5 alkene  
119 triols, 2-methylglyceric acid, 3-hydroxyglutaric acid and levoglucosan. Terpenoic acids and  
120 organic markers are included to assist in characterizing the extent of biogenic compound  
121 oxidation and atmospheric processing (i.e., aerosol aging) as well as contributions from biomass  
122 burning sources. Aerosol bulk chemical measurements are conducted to estimate total water  
123 soluble organic N and C concentrations. Characterization of seasonal patterns in concentrations  
124 of organic N species and assessment of potential sources and formation processes are  
125 emphasized.

126

## 127 **2. Experimental methods and materials**

### 128 **2.1 Sampling site and atmospheric aerosol collection**



129        The study was conducted at the U.S. Forest Service Coweeta Hydrologic Laboratory, a  
130        2185-ha experimental forest in southwestern, North Carolina, USA (35°3' N, 83°25' W) near the  
131        southern end of the Appalachian Mountain chain. The climate is classified as maritime, humid  
132        temperate, with mean monthly temperatures ranging from 3.3°C in January to 21.6°C in July  
133        (Swift et al., 1988). Elevation ranges from 675 to 1592 m with a corresponding range in annual  
134        precipitation of 1800 to 2500 mm (Swank and Crossley, 1988). The vegetation is characterized  
135        as mixed coniferous/deciduous including oak, pines, and hardwoods (Bolstad et al, 1998).  
136        Atmospheric measurements were conducted in the lowest part of the basin (686 m), collocated  
137        with long term measurements of air and precipitation chemistry conducted by CASTNET and  
138        NADP networks, respectively.

139        The sampling site is 5 km west of Otto, NC (population 2500) and Highway 23 (Figure  
140        S1, supplemental material). Land to the north, west and south of Coweeta is undeveloped forest.  
141        Typical rural development is present to the east of the site, consisting of houses and small scale  
142        farming for hay and crop production including some scattered cow and horse pastures. The  
143        nearest metropolitan areas include Atlanta, Georgia (175 km southwest), Chattanooga,  
144        Tennessee (175 km west), Knoxville, Tennessee (110 km north/northwest), Asheville, North  
145        Carolina (100 km northeast), and Greenville, South Carolina (100 km southeast). The location  
146        of the sampling site within the context of NO<sub>x</sub> and SO<sub>2</sub> point sources in the eastern U.S. is  
147        shown in supplemental material (Figure S2). Only minor point sources are present within ~ 100  
148        km of the site.

149        The study period summarized here comprises three seasonal intensives conducted during  
150        the spring, summer and fall of 2015. Each campaign was conducted for approximately 3 weeks  
151        (21 May to 9 June, 6 August to 25 August, 9 October to 26 October). A high-volume Tisch TE-  
152        1000 (Tisch Environmental, Cleves, OH) dual cyclone PM<sub>2.5</sub> sampler operated at a flow rate of  
153        230 L/min was set up on the ground to collect 24 hr (started at 7am local time) integrated  
154        samples on pre-baked (550°C for 12hrs) quartz fiber (QF) filters (90mm, Pall Corporation, Port  
155        Washington, NY). Field blanks were collected the same way except being loaded in the sampler  
156        without the pump switched on. A total of 58 ambient samples and 10 field blanks were obtained.  
157        Collected filter samples were transferred back to the laboratory in a cooler and stored in a freezer  
158        at -20 °C before chemical analysis.

## 159        2.2 Trace gas and meteorological measurements



During the spring 2015 campaign, NO<sub>x</sub> concentrations were measured on a short tower (7 m above ground) co-located with the CASTNET and high volume PM samplers. NO<sub>x</sub> concentrations were measured using a commercial NO-NO<sub>2</sub>-NO<sub>x</sub> analyzer (model 42S, Thermo Environmental Instruments, Incorporated, Franklin, MA). Briefly, nitric oxide (NO) is measured directly on one channel by chemiluminescence. On a 2<sup>nd</sup> channel, NO<sub>2</sub> is converted to NO by a molybdenum catalyst heated to 325°C, yielding the concentration of NO<sub>x</sub> (NO + NO<sub>2</sub>). This approach may overestimate NO<sub>x</sub> since other oxidized nitrogen gases such as HNO<sub>3</sub>, PAN and HONO could also be reduced to NO on the heated molybdenum surface (Fehsenfeld et al., 1987; Williams et al., 1998; Zellweger et al., 2000). However, the use of an inlet filter and approximately 12 m of sample line between the atmospheric inlet and converter likely minimized the potential bias from HNO<sub>3</sub>. For subsequent campaigns, NO<sub>x</sub> concentrations were estimated from a co-located NO<sub>y</sub> analyzer. Similar to the NO<sub>x</sub> instrument, NO<sub>y</sub> and HNO<sub>3</sub> were also measured using a modified model 42S NO-NO<sub>2</sub>-NO<sub>x</sub> analyzer. The NO<sub>y</sub> technique is described in detail by Williams et al. (1998). Briefly, total oxidized reactive nitrogen (NO<sub>y</sub>) is converted to NO using a molybdenum catalyst heated to 325°C. On a 2<sup>nd</sup> channel, a metal denuder coated with potassium chloride (KCl) is used to remove HNO<sub>3</sub> before passing through a 2<sup>nd</sup> molybdenum converter heated to 325°C. The difference between the total NO<sub>y</sub> measurement and the HNO<sub>3</sub>-scrubbed NO<sub>y</sub> measurement is interpreted as HNO<sub>3</sub>. NO<sub>x</sub> concentrations were estimated from the differences between measured NO<sub>y</sub> and HNO<sub>3</sub>, which provided an upper bound estimation as gaseous N containing species were not excluded (eg. PAN and organic nitrates). Hourly ozone concentrations were measured by CASTNET (U.S. EPA, 2017) on a co-located 10m tower. Hourly meteorological data were provided by CASTNET (U.S. EPA, 2017) and Forest Service (Miniat et al 2015; Oishi et al., 2017), including temperature, relative humidity, solar radiation and precipitation.

184

## 185 2.3 Chemical analysis

### 186 2.3.1 Elemental and organic carbon analysis

187 A 1.5cm<sup>2</sup> QF punch was analyzed for elemental carbon (EC) and organic carbon (OC) using  
188 a thermo-optical transmittance (TOT) method (Sunset Laboratory Inc, Oregon, USA) (Birch and  
189 Cary, 1996).



### 2.3.2 Water soluble species by Ion Chromatography (IC) and Total Organic Carbon/Total Nitrogen (TOC/TN) analyzers

A second QF punch (1.5 cm<sup>2</sup>) from each sample was extracted with DI water (18.2 MΩ·cm, Milli-Q Reference system, Millipore, Burlington, MA) in an ultrasonic bath for 45 min. The sample extract was filtered through a 0.2 μm pore size PTFE membrane syringe filter (Iso-disc, Sigma Aldrich, St. Louis, MO) before subsequent analyses.

Water soluble organic carbon (WSOC) and total N (WSTN) concentrations were measured using a chemiluminescence method that included a total organic carbon analyzer (TOC-Vcsh) combined with a total nitrogen module (TNM-1) (Shimadzu Scientific Instruments, Columbia, MD). For WSOC measurements, 25% phosphoric acid was mixed with sample extract (resulting in a 1.5% acid mixture) and sparged for 3 min to remove any existing carbonate/bicarbonate.

Inorganic species (NH<sub>4</sub><sup>+</sup>, NO<sub>3</sub><sup>-</sup>, NO<sub>2</sub><sup>-</sup> and SO<sub>4</sub><sup>2-</sup>) were analyzed using ion chromatography (IC, Dionex model ICS-2100, Thermo Scientific, Waltham, MA). The IC was equipped with guard (IonPac 2mm AG23) and analytical columns (AS23) for anions. The samples were analyzed using an isocratic eluent mix carbonate/bicarbonate (4.5/0.8 mM) at a flow rate of 0.25 mL/min. Cations were analyzed by Dionex IonPac 2mm CG12 guard and CS12 analytical columns; separations were conducted using 20 mM methanesulfonic acid (MSA) as eluent at a flow rate of 0.25 mL/min. Multi-point (≥5) calibration was conducted using a mixture prepared from individual inorganic standards (Inorganic Ventures, Christiansburg, VA). A mid-level accuracy check standard was prepared from certified standards mix (AccuStandard, New Haven, CT) for quality assurance/quality control purposes.

### 2.3.3 UV-Vis light absorption analysis

Several studies have shown that methanol can extract aerosol OC at higher efficiencies than water, and that a large fraction of light absorption in the near-UV and visible ranges is ascribed to water insoluble OC (Chen and Bond, 2010; Liu et al., 2013; Cheng et al., 2016). In this study, a QF punch (1.5 cm<sup>2</sup>) was extracted with 5 mL methanol (HPLC grade, Thermo Fisher Scientific Inc.) in a tightly closed amber vial, sonicated for 15 min, and then filtered through a 0.2 μm pore size PTFE filter (Iso-disc, Sigma Aldrich, St. Louis, MO). The light absorption of filtered extracts was measured with a UV-Vis spectrometer over λ = 200-900 nm at





221 0.2 nm resolution (V660, Jasco Incorporated, Easton MD). The wavelength accuracy is less than  
222  $\pm 0.3$  nm; the wavelength repeatability is less than  $\pm 0.05$  nm. A reference cuvette containing  
223 methanol was used to account for solvent absorption. The UV-Vis absorption of field blank  
224 samples was negligible compared to ambient samples, but used for correction nonetheless. For  
225 ease of analysis, the absorption at 365 nm referencing to absorption at 700 nm was used as a  
226 general measure of the absorption by all aerosol chromophore components (Hecobian et al.,  
227 2010).

228

#### 229 2.3.4. Analysis of isoprene and monoterpene SOA markers and anhydrosugars by GC-MS

230 Aliquots of each filter (roughly  $\frac{1}{4}$ ) were extracted by 10 mL of methanol and methylene  
231 chloride mixture (1:1, v/v) ultrasonically twice (15 minutes each). The total extract was filtered  
232 and concentrated to a final volume of  $\sim 0.5$  mL. Next, extracts were transferred to a 2 mL glass  
233 vial and concentrated to dryness under a gentle stream of ultrapure  $N_2$  and reacted with 50  $\mu$ L of  
234 N, O-bis(trimethylsilyl)trifluoroacetamide (BSTFA) containing 1% trimethylchlorosilane  
235 (TMCS) and 10  $\mu$ L of pyridine for 3 h at 70 °C. After cooling down to room temperature,  
236 internal standards (mixture of 17.6 ng  $\mu$ L<sup>-1</sup> acenaphthalene-d10 and 18.6 ng  $\mu$ L<sup>-1</sup> pyrene-d4  
237 mixed in hexane) and pure hexane were added. The resulting solution was analyzed by an  
238 Agilent 6890N gas chromatograph (GC) coupled with an Agilent 5975 mass spectrometer (MS)  
239 operated in the electron ionization mode (70 eV). An aliquot of 2  $\mu$ L of each sample was injected  
240 in splitless mode. The GC separation was carried out on a DB-5 ms capillary column (30 m  $\times$   
241 0.25 mm  $\times$  0.25  $\mu$ m, Agilent Technologies, Santa Clara, CA). The GC oven temperature was  
242 programmed from 50 °C (hold for 2 min) to 120 °C at 30 °C min<sup>-1</sup> then ramped at 6 °C min<sup>-1</sup> to  
243 a final temperature of 300 °C (hold for 10 min). Linear calibration curves were derived from six  
244 dilutions of quantification standards. Anhydrosugars (levoglucosan) were quantified using  
245 authentic standard; 2-methyltetrols (2-methylthreitol and 2-methylerythritol) and C-5 alkene  
246 triols were quantified using meso-erythritol; other SOA tracers (e.g., hydroxyl dicarboxylic acid)  
247 were quantified using cis-ketopinic acid (KPA) (refer to supplemental information Table S1).  
248 The species not quantified using authentic standards were identified by the comparison of mass  
249 spectra to previously reported data (Claeys, et al., 2004, 2007; Surratt et al., 2006; Kleindienst et  
250 al., 2007). Field blanks were collected and no contamination was observed for identified species.

251





2.3.5. Analysis of organosulfates, terpenoic acids and nitro-aromatics by High Performance Liquid Chromatography- electrospray ionization-Quadrupole time-of-flight-Mass Spectrometer (HPLC-ESI(-)-QTOF-MS)

Approximately 3-5 mL of methanol was used to ultrasonically extract (twice for 15 min) roughly half of each 90mm QF sample. Internal standards (I.S.) were spiked onto each filter sample prior to extraction (refer to Table S2, S3 and S4 for individual compounds and surrogate standards used for each group of compounds). Extracts were filtered into a pear-shaped glass flask (50 mL) and rotary evaporated to ~0.1 mL. The concentrated extracts were then transferred into a 2 mL amber vial that was rinsed with methanol 2-3 times. The final sample extract volume was ~500 µL prior to analysis. All the glassware used during the extraction procedure was pre-baked at 550°C overnight. Extracted samples were stored at or below -20 °C prior to analysis and typically analyzed within 7 d.

An HPLC coupled with a quadrupole time-of-flight mass spectrometer (1200 series LC and QTOF-MS, Model 6520, Agilent Technologies, Palo Alto, CA) was used for target compound identification and quantification. The QTOF-MS instrument was equipped with a multimode ion source operated in electrospray ionization (ESI) negative (-) mode. Optimal conditions were achieved under parameters of 2000 V capillary voltage, 140 V fragmentor voltage, 65 V skimmer voltage, 300 °C gas temperature, 5 L/min drying gas flow rate and 40 psig nebulizer. The ESI-QTOF-MS was operated over the m/z range of 40 to 1000 at a 3 spectra/s acquisition rate. Target compounds separation was achieved by a C18 column (2.1×100 mm, 1.8 µm particle size, Zorbax Eclipse Plus, Agilent Technologies) with an injection volume of 2 µL and flow rate of 0.2 mL/min. The column temperature was kept at 40 °C, and gradient separation was conducted with 0.2% acetic acid (v:v) in water (eluent A) and methanol (eluent B). The eluent B was maintained at 25% for the first 3 min, increased to 100% in 10 min, held at 100% from 10 to 32 min, and then dropped back to 25% from 32 to 37 min, with a 3 min post run time. During each sample run, reference ions were continuously monitored to provide accurate mass corrections (purine and HP-0921 acetate adduct, Agilent G1969-85001). Typically, the instrument exhibited 2 ppm mass accuracy. Tandem MS was conducted by targeting ions under collision-induced dissociation (CID) to determine parent ion structures. Agilent software Mass hunter was used for data acquisition (Version B05) and for further data analysis (Qualitative and Quantitative Analysis, Version B07). The mass accuracy for compound



283 identification and quantification was set at  $\pm 10$  ppm. Calibration curves were generated from  
284 diluted standard compound mixtures. Recoveries of the extraction and quantification were  
285 performed by spiking known amounts of standards to blank QF filters. Then the spiked blank  
286 filters were extracted and analyzed the same way as ambient collected samples. The average  
287 recoveries of standard compounds are listed in supplemental information Table S5 and ranged  
288 from  $75.2 \pm 5.6$  to  $129.4 \pm 4.2\%$ . Isomers were identified for several compounds, no further  
289 separation was conducted and combined total concentrations are reported in this study.

290

#### 291 2.4 Source apportionment by Positive Matrix Factorization

292 Positive Matrix Factorization (PMF) was used to identify potential sources of compounds  
293 measured at Coweeta. Here we use the PMF2 model (Paatero, 1998a, b) coupled with a bootstrap  
294 technique (Hemann et al., 2009), which has been applied in a number of previous studies (Xie et  
295 al., 2012, 2013, 2014,). Briefly, PMF resolves factor profiles and contributions from a series of  
296 PM compositional data with an uncertainty-weighted least-squares fitting approach; the coupled  
297 stationary bootstrap technique generates 1000 replicated data sets from the original data set and  
298 each was analyzed with PMF. Normalized factor profiles were compared between the base case  
299 solution and bootstrapped solutions, so as to generate a factor matching rate. The determination  
300 of the factor number was based on the interpretability of different PMF solutions (3-6 factors)  
301 and factor matching rate ( $>50\%$ ). Detailed data selection criteria are presented in supplemental  
302 information.

303

### 304 3. Results and discussion

#### 305 3.1 Meteorology, NO<sub>x</sub>, and O<sub>3</sub>

306 Statistics of atmospheric chemistry and meteorological measurements are summarized by  
307 season in Table 1. In general, the sampling site was humid and cool, even in the summer, with  
308 an average summer temperature of  $\sim 21^\circ\text{C}$  and RH of 82%. During the fall, much lower  
309 temperature ( $\sim 12^\circ\text{C}$ ) and less humid conditions (RH=78%) were observed. NO<sub>x</sub> concentrations  
310 were generally less than 1 ppb, which is considered typical for such a remote forest site removed  
311 from major emission sources.

312 [O<sub>3</sub>] was generally low (Table 1) with seasonal averages of 15 ppb to 25 ppb. Historical  
313 seasonal [O<sub>3</sub>] over the past 5 years (2011 to 2015) are shown in supplemental information Figure



S3. A spring maximum in  $[O_3]$  is typically observed at this site, with lower concentrations during summer. Seasonal clustered back trajectories (Figure S4 in supplemental information) suggest that during spring the Coweeta sampling site was under the influence from air masses transported from Atlanta urban areas. In addition, a spring maximum  $[O_3]$  may be due to higher chemical consumption of  $O_3$  by reactive monoterpenes and sesquiterpene emitted in the forest. With observed relatively moderate summer temperatures and generally low  $[NO_x]$ , the site also experiences frequent cloud cover in summer lowering the intensity of solar radiation which may suppress ozone production relative to spring conditions. Additionally, deposition of  $O_3$  to the forest would be expected to peak during the summer, when leaf area is greatest.  $O_3$  correlates positively with  $NO_x$  in summer and fall but not spring, indicating  $O_3$  production might be relatively more VOC-limited in spring than the other seasons in this region.

325

### 3.2 Bulk water soluble organic nitrogen and carbon

Water soluble bulk organic N (WSON) was estimated as the difference between WSTN and the sum of the inorganic N species ( $NH_4^+$ ,  $NO_3^-$  and  $NO_2^-$ ). Nitrogen component contributions to WSTN are presented in Figure 1a, which shows  $NH_4^+$  as the most abundant component, contributing  $85 \pm 11\%$  w/w to total WSTN mass. The oxidized inorganic N components ( $NO_3^-$  and  $NO_2^-$ ) accounted for less than 2% w/w of WSTN measured. Such a small contribution of  $NO_3^-$  to inorganic N (typically  $<10\%$  of inorganic N ( $NO_3^- + NH_4^+$ )) in  $PM_{2.5}$  is consistent with long term CASTNET measurements at Coweeta. The average contribution of WSON to WSTN over the entire study period was  $14 \pm 11\%$  w/w. This fraction reached a maximum of  $\sim 18\%$  w/w in the spring (average) and minimum of  $\sim 10\%$  in the fall (average), exhibiting pronounced seasonal variability. Within individual samples (Figure 1b), values ranged from near zero to 45%. Our study wide average of 14% falls within the range of measurements at North American forest sites, including Duke Forest, North Carolina ( $\sim 33\%$ , Lin et al., 2010) and Rocky Mountain National Park (14-21%) (Benedict et al., 2012).

WSOC accounted for roughly  $62 \pm 13\%$  of OC throughout the entire study period with no significant seasonal variability. A time series of OC and WSOC along with temperature and precipitation is presented in Figure 1c. On average, OC concentrations increased during warmer spring and summer seasons and decreased when the temperature decreased in fall. Concentrations of OC were positively correlated with temperature ( $r=0.30$ ,  $p<0.05$ ), presumably



345 in response to emissions of biogenic precursors and formation of secondary organic aerosols by  
346 photooxidation. Spring and summer were generally moist and warm with frequent precipitation  
347 (relative humidity presented in Table 1). Precipitation events corresponded to decreasing OC and  
348 WSOC concentrations demonstrating the scavenging effect due to wet deposition.

349 Spearman rank correlation coefficients among measured species and meteorological  
350 variables as well as other gas phase measurements are presented in Table 2 for each season  
351 ( $p < 0.01$  for values in bold). As expected,  $\text{NH}_4^+$  and  $\text{SO}_4^{2-}$  tracked well over each season ( $r > 0.9$ ,  
352  $p < 0.01$ ).  $\text{NH}_4^+$  was mainly associated with  $\text{SO}_4^{2-}$  given the fact that  $\text{NO}_3^-$  and  $\text{NO}_2^-$  were  
353 generally negligible compared to  $\text{SO}_4^{2-}$ . WSOC is often used as an SOA surrogate and accounts  
354 for a significant portion (62% w/w) of OC during all sampling periods. WSOC correlated  
355 strongly with OC over both summer and fall ( $r > 0.95$ ,  $p < 0.01$ ), but less so during spring ( $r = 0.74$ ,  
356  $p < 0.01$ ). WSOC also positively correlates with WSON over spring and fall ( $r > 0.75$ ,  $p < 0.01$ ) but  
357 less so during summer ( $r = 0.5$ ,  $p > 0.01$ ). Note that both [WSOC] and [OC] are highest in the  
358 summer, which likely indicates higher biogenic emissions and SOA formation. However, the  
359 weak WSON-WSOC correlation suggests a variety of source contributions over the different  
360 seasons. [EC] was negligible over the entire study except a modest spike at the end of October  
361 when wood burning was the most likely the source. Details of this event are discussed in the  
362 subsequent sections.

363

364

### 365 3.3 Nitro-aromatics

366 Concentrations of nitro-aromatics, organosulfate/nitrooxy-organosulfate, and terpenoic  
367 acids are summarized in Tables 3, S2, S3 and S4. A time series of compound class totals are  
368 presented in Figure 2. Generally negligible concentrations of nitro-aromatics were observed  
369 during spring and summer except for occasional spikes. However, higher concentrations of nitro-  
370 aromatics were observed in the fall when moderate correlations were observed with levoglucosan  
371 (Figure 3,  $r \geq 0.5$ ,  $p < 0.01$ ; see table SI 6 for correlation coefficients). A residential wood burning  
372 contribution is likely given the lower temperatures observed during this season. Similar positive  
373 correlations between nitro-aromatics and wood burning are also reported during the winter  
374 season (Gaston et al., 2016; Kahnt et al., 2013; Kitanovski et al., 2012; Iinuma et al., 2010,  
375 2016). Smoke at the sampling site on October 19<sup>th</sup> and 21<sup>st</sup> coincided with firewood burning at



the main office of the Coweeta Hydrologic Laboratory, immediately adjacent to the sampling location. Nitro-aromatics were relatively elevated, but no significant increase in organosulfates or terpenoid acids were found from these fresh smoke events. In contrast, an example of an aged biomass burning signal is illustrated on October 24<sup>th</sup> and 25<sup>th</sup>. Pronounced spikes of nitrocatechol(C<sub>6</sub>H<sub>5</sub>NO<sub>4</sub>), methyl-nitrocatechol(C<sub>7</sub>H<sub>7</sub>NO<sub>4</sub>) and levoglucosan were observed (Figure 3), along with elevated concentrations of organosulfates, OC and aged biogenic aerosol tracers (terpenoid acids m/z 203 and 187 shown in Figure 4a, detailed discussion can be found in the subsequent section). However, EC was only slightly higher. This event did not correspond to local burning at Coweeta and was most likely associated with long range transport.

Nitro-aromatics correlate with EC across the seasons; both are likely emitted from biomass burning (Gaston et al., 2016; Iinuma et al., 2010; Kahnt et al., 2013; Mohr et al., 2013). Interestingly, light absorption at  $\lambda=365\text{nm}$  is highly correlated ( $r=0.80$ ,  $p<0.01$ ) with nitro-aromatics in the fall when nitro-aromatic concentrations were elevated. In addition, NO<sub>x</sub> correlates inversely ( $r=-0.72$ ,  $p<0.01$ ) with temperature in the fall. Lower fall temperatures in the region may have resulted in frequent residential wood burning, which emits NO<sub>x</sub> and light absorbing BrC (eg. nitro-aromatics) (Liu et al., 2015; Mohr et al., 2013). Although nitro-aromatics account for a minor fraction of OM, they could potentially contribute to 4% of light absorption by BrC (Mohr et al., 2013). Overall, nitro-aromatics displayed relatively weak correlation with WSON ( $r<0.65$ ) across all seasons; the extreme low concentrations observed suggest a generally small contribution of nitro-aromatics to WSON at the sampling site, hence the lack of strong correlation.

### 3.4 Organosulfates and nitrooxy-organosulfates

Organosulfate concentrations were highest in summer and lowest in fall (Table 3), contributing 3.9 and 1.0 % w/w of organic matter (OM, estimated by applying an OM/OC factor of 2) mass, respectively, during these seasons. Organosulfate formation is an example of heterogeneous chemistry involving uptake of reactive precursors on acidified sulfate aerosols requiring a mixture of biogenic and anthropogenic emissions. The air masses at Coweeta are mainly from the southwest and westerly directions in spring and summer, but during fall may become more stagnant and slow moving during southwesterly conditions or shift to the northwest (see clustered back trajectories are shown in Figure S4). Because Atlanta, GA is southwest of



407 Coweeta, southwesterly flow during spring and summer may be associated with long range  
408 transport of urban pollutants and precursors, including sulfate and sulfuric acid, leading to  
409 elevated organosulfate formation compared to fall when the prevailing wind direction changes.

410 Among all organosulfates identified, the isoprene derived organosulfate ( $m/z$  215, 2-  
411 methyltetrol derived), which is formed from isoprene derived epoxydiols (IEPOX) under low  
412  $\text{NO}_x$  conditions, was the most abundant; concentrations reached  $167 \text{ ng/m}^3$  in summer. Similar  
413 high concentrations were also reported in ambient samples collected at other sites in the  
414 southeastern U.S. (Lin et al., 2013b; Worton et al., 2013). Of the six nitrooxy-organosulfates  
415 identified, isoprene derived  $m/z$  260 was most abundant, approximately 6-fold higher than  
416 monoterpene derived  $m/z$  294 nitrooxy-organosulfate.

417 A subset of possible organosulfates and nitrooxy-organosulfates produced from isoprene  
418 and monoterpene oxidation exhibit strong correlations with distinctive SOA tracers (eg. markers  
419 2-methylglyceric acid, C-5 alkene triols and methyltetrols for isoprene oxidation products; tracer  
420 3-Hydroxyglutaric acid for pinene oxidation products) (see table SI 7). Lack of correlation  
421 between nitrooxy-organosulfate  $m/z$  294 and 3-hydroxyglutaric acid may indicate a nighttime  
422 nitrate radical formation pathway rather than photochemical oxidation. Given that  $\text{NO}_x$  levels at  
423 the rural Coweeta sampling site were typically less than 1 ppb, photo-oxidation pathways  
424 involving high  $[\text{NO}_x]$  to form nitrooxy-organosulfates are not likely. Nighttime nitrate radical  
425 chemistry is the most likely formation mechanism under such conditions. In contrast to our  
426 observations, He et al. (2014) report good correlations ( $r>0.5$ ,  $p<0.01$ ) of  $m/z$  294 with 3-  
427 hydroxyglutaric acid and higher daytime  $m/z$  294 concentrations for summer samples collected  
428 in Pearl River Delta, China, where a seasonal average  $\text{NO}_x$  level of 30 ppb was observed. The  
429 authors suggested that the dominant  $m/z$  294 formation pathway was through daytime  
430 photochemistry rather than nighttime  $\text{NO}_3$  chemistry. The extremely low  $\text{NO}_x$  levels at our study  
431 site compared to that measured by He et al. may explain the opposite behavior in terms of  $m/z$   
432 294 formation mechanisms.

433 Organosulfates exhibited statistically significant correlations with WSON only in the  
434 summer ( $r=0.64$ ,  $p<0.01$ ), which reflected the importance of N containing organosulfates or their  
435 formation chemistry to WSON. During this season, nitrooxy-organosulfates accounted for ~2%  
436 of bulk WSON, on average. A strong correlation may therefore not be expected.

437



### 3.5 Terpenoic acids

Terpenoic acids, which provide insight into the extent of biogenic compound oxidation and atmospheric processing (i.e., aerosol aging), were the most abundant group of compounds relative to nitro-aromatics and organosulfates. On average, terpenoic acids accounted for 6.5 to 8.7% w/w of OM in PM<sub>2.5</sub>. The warmer spring and summer periods show higher production of terpenoic acids compared to the cool and drier fall season. Higher emissions of biogenic VOC precursors as well as higher solar radiation intensities during warm seasons, which drive photochemistry, are factors contributing to observed seasonal variability.

The terpenoic acids correlate well with WSOC and OC (Table 2). This is expected as terpenoic acids account for a substantial portion of OM at the site. Individual acids (except compounds C<sub>7</sub>H<sub>10</sub>O<sub>4</sub> and C<sub>9</sub>H<sub>14</sub>O<sub>4</sub>) exhibit strong correlations with the pinene derived SOA tracer 3-hydroxyglutaric acid ( $r > 0.75$ ,  $p < 0.01$ ; correlation coefficients shown in the supplemental information Table S8), indicating the presence of  $\alpha$ -/ $\beta$ -pinene oxidation products. The poor correlations between acids C<sub>7</sub>H<sub>10</sub>O<sub>4</sub> ( $m/z$  157) and C<sub>9</sub>H<sub>14</sub>O<sub>4</sub> ( $m/z$  185) suggests the presence of biogenic VOC precursors other than  $\alpha$ -/ $\beta$ -pinene, such as limonene and  $\Delta^3$ -carene (Gomez-Gonzalez et al., 2012).

Recent chamber studies identified several terpenoic acid structures also observed in ambient aerosol samples, including 3-methyl-1,2,3-butanetricarboxylic acid (MBTCA, C<sub>8</sub>H<sub>12</sub>O<sub>6</sub>,  $m/z$  203), 2-hydroxyterpenylic acid (C<sub>8</sub>H<sub>12</sub>O<sub>5</sub>,  $m/z$  187), terpenylic acid (C<sub>8</sub>H<sub>12</sub>O<sub>4</sub>,  $m/z$  171) and diaterpenylic acid acetate (DTAA, C<sub>10</sub>H<sub>16</sub>O<sub>6</sub>,  $m/z$  231) (Claeys et al., 2009; Kahnt et al., 2014). MBTCA and 2-hydroxyterpenylic acid have been identified as highly oxygenated, higher generation  $\alpha$ -pinene SOA markers, and observed in high abundance in ambient aerosols (Gomez-Gonzalez et al., 2012; Kahnt et al., 2014; Muller et al., 2012; Szmigielski et al., 2007). Additionally, terpenylic acid and DTAA are characterized as early photooxidation products from  $\alpha$ -pinene ozonolysis. Claeys et al. (2009) proposed further oxidation processes (aging) of terpenylic acid involving OH radical chemistry to form 2-hydroxyterpenylic acid. Figure 4 provides a time series of the terpenoic acids identified in this study. In general, 2-hydroxyterpenylic acid was the most abundant species across the seasons. To assess the extent of aging, concentration ratios of higher generation oxidation products (C<sub>8</sub>H<sub>12</sub>O<sub>6</sub>,  $m/z$  203 and C<sub>8</sub>H<sub>12</sub>O<sub>5</sub>,  $m/z$  187) to early oxidation fresh SOA products (C<sub>8</sub>H<sub>12</sub>O<sub>4</sub>,  $m/z$  171 and C<sub>10</sub>H<sub>16</sub>O<sub>6</sub>,  $m/z$  231) are calculated. Estimated seasonal averages of these ratios are 3.98, 4.37 and 2.44 for





469 spring, summer and fall, respectively. Thus, during spring and summer, aerosols observed at the  
470 site were more aged. Figure 4 shows the correlation of these ratios with temperature ( $r=0.79$ ,  
471  $p<0.001$ ) and solar radiation ( $r=0.23$ ,  $p<0.1$ ). A clear relationship between temperature and OH  
472 radical initiated oxidation (aging) is evident. However, oxidation appears less dependent on solar  
473 radiation at our sampling site. Similar higher contribution of these aged biogenic SOA tracers  
474 was also reported under warm summer conditions characterized by high temperature and high  
475 solar radiation (Claeys et al., 2012; Gomez-Gonzalez et al., 2012; Hamilton et al., 2013; Kahnt et  
476 al., 2014).

477 Terpenoic acids may also provide some insight into the formation mechanisms of  
478 organosulfates. While organosulfate concentrations are highest during summer, correlations with  
479  $\text{SO}_4^{2-}$  are strongest during spring and fall and weakest during summer. Conversely,  
480 organosulfates and terpenoic acids correlate strongly ( $r=0.91$ ,  $p<0.01$ ) during summer.  
481 Terpenoic acids are either first or second generation oxidation products from gas phase  
482 monoterpenes; particulate  $\text{SO}_4^{2-}$  abundance should not substantially influence the gas-particle  
483 partitioning of terpenoic acids. The strong correlation between organosulfates and terpenoic  
484 acids in summer suggests organosulfate formation is limited by monoterpene emissions rather  
485 than  $\text{SO}_4^{2-}$  availability while in the spring and fall (especially fall), organosulfate production may  
486 be more limited by  $\text{SO}_4^{2-}$ . Degree of particle neutralization, calculated as the molar ratio of  $\text{NH}_4^+$   
487 to the sum of  $\text{SO}_4^{2-}$  and  $\text{NO}_3^-$ , averaged 0.94, 0.98 and 0.94 for spring, summer and fall,  
488 respectively. Neutralization being close to but less than unity implies that aerosols are slightly  
489 acidic at the site. Chamber studies have illustrated that acidified  $\text{SO}_4^{2-}$  could enhance  
490 heterogeneous reactions to form SOA from isoprene and monoterpenes (Iinuma et al., 2009;  
491 Surratt et al., 2007, 2010). Similar positive correlations observed at the Coweeta site were also  
492 found between isoprene tracers including isoprene derived organosulfates and  $\text{SO}_4^{2-}$  by Lin et al.  
493 (2013b) at a rural site in the southeastern U.S. However, in contrast to chamber experiments, this  
494 study and other ambient field measurements have not provided clear evidence of acidity  
495 enhancement of organosulfate formation (He et al., 2014; Lin et al., 2013b; Worton et al., 2011),  
496 indicating possible differences in exact mechanisms and processing to form these organosulfates  
497 under atmospheric conditions relative to chamber studies. Recent mechanistic modeling  
498 simulations by Budisulistiorini et al., (2017) suggest that the role of sulfate on IEPOX-



organosulfates formation might be through surface area uptake of IEPOX and rate of particle phase reaction.

Very good correlations between WSON and terpenoic acids were observed during summer and fall ( $r \geq 0.7$ ,  $p < 0.01$ ). Given the secondary nature of terpenoic acids, this finding may suggest that WSON during these two seasons is associated with more aged air masses and perhaps dominated by secondary organic components rather than primary emitted N containing constituents such as pollens, fungi and bacteria (Elbert et al., 2007; Miyazaki et al., 2014).

### 3.6 Contribution of identified N containing species to WSTN and WSON

Nitro-aromatics and nitrooxy-organosulfates were estimated to account for as much as 28% of WSON, which reflected the abundance and potential importance of these groups of species to the atmospheric N deposition budget. Seasonal average ratios of identified WSON to WSTN ranged from 1.0 to 4.4% with the highest recorded for fall (Table 4). Nitrooxy-organosulfates dominated over nitro-aromatics as a source of organic nitrogen, contributing > 90% to identified WSON across seasons. However, during episodes of biomass burning, nitro-aromatics contribute as much as 32% of identified WSON compounds. The ratio of WSON to WSOC was estimated to be 0.05, 0.04 and 0.02 for spring, summer and fall, which implies organic N being most enriched during spring, reflecting a spring maximum in seasonal emissions of Organic N from biological sources (e.g. pollens, spores, leave litter decomposition) combined with smaller contributions from secondary atmospheric processes. The observed N/C ratios in this study were slightly lower than those reported for other forest sites (0.03-0.09) (Lin et al., 2010; Miyazaki et al., 2014), which are not as remote and pristine as the forest site in this study. Anthropogenic influences at the study sites described by Lin et al. (2010) and Miyazaki et al. (2014) such as  $[\text{SO}_4^{2-}]$  and  $[\text{NO}_x]$  were  $\sim 5$  times higher than those measured at the Coweeta site. Concentration weighted average N/C ratios for identified compounds (nitro-aromatics, organosulfates/nitrooxy-organosulfates and terpenoic acids) in this study were estimated to be 0.003. This value is 10 times less than the overall N/C ratio observed at the site, which indicates existence of other higher N content species in the aerosols.

### 3.7 PMF analysis

PMF analysis was conducted to identify individual source contributions to total WSOC. Factor profiles and time series of factor contributions are presented in figures 5 and 6. Listed in



order of percent contribution to WSOC, the five factors which were resolved include secondary sulfate processing (35.3%), isoprene SOA (24.3%), WSON containing OM (20.0%), biomass burning (15.1%) and monoterpene SOA (5.2%). Overall, these factors could explain  $89 \pm 2\%$  of observed WSOC ( $r=0.88$ ,  $p<0.0001$ ). The secondary sulfate profile contained a signature of high  $\text{SO}_4^{2-}$ , which was most likely present as fine particulate  $(\text{NH}_4)_2\text{SO}_4$  and  $\text{NH}_4\text{HSO}_4$ . Secondary sulfate was the most important factor during spring, though was a significant contributor in summer and fall as well. Isoprene SOA, which was identified based on isoprene derived organosulfates and isoprene SOA markers, was the most important factor during summer. The biomass burning factor, which exhibited a high portion of nitro-aromatic and levoglucosan markers, dominated in the fall. This pattern agreed well with observed patterns of nitro-aromatic compounds. Monoterpene SOA, which was resolved based on the composition of monoterpene derived organosulfates, was overall a minor contributor with the exception of a few samples during the fall intensive.

WSON containing OM contributed 20% to WSOC, overall, demonstrating a significant association between organic N and C in  $\text{PM}_{2.5}$  at our study site. The WSON containing OM source profile exhibited weak correlation with most measured species with the exception of modest correlations with terpenoic acids. WSON containing OM contributed more to WSOC in late spring and early summer, which was consistent with observed higher production of nitrooxy-organosulfates during these sampling periods as well as terpenoic acids. The relationship with terpenoic acids may reflect an association of WSON with more aged air masses. Because nitro-aromatics and nitrooxy-organosulfates contribute only a small portion of WSON, on average, the 20% contribution of WSON containing OM to WSOC primarily reflects the contribution of organic N present in bulk WSON but unspicated in this work.

#### 4. Conclusions

Ambient  $\text{PM}_{2.5}$  collected at a temperate mountainous forest site were investigated on a bulk chemical and a molecular level during spring, summer, and fall of 2015. Analyses focused on speciation of nitro-aromatics associated with biomass burning, organosulfates produced from biogenic SOA precursors, and terpenoic acids formed from monoterpene oxidation. Among these three groups, terpenoic acids were estimated to be most abundant, contributing up to a seasonal average of 8.7% of OM in  $\text{PM}_{2.5}$  during spring. Warm periods in spring and summer exhibited



561 highest production of terpenoic acids, when SOA correspondingly showed a higher degree of  
562 aging. Relative abundance of aged biogenic SOA tracers (MBTCA and 2- hydroxyterpenylic  
563 acid), which reflect the degree of organic aerosol aging, showed a strong correlation with  
564 temperature. Such a relationship might indicate temperature dependence of OH radical initiated  
565 oxidation steps or aging in the formation of higher generation oxidation products.

566 Organosulfates showed a peak in summer and lowest concentrations during fall,  
567 contributing averages of 3.9 and 1.0 % of OM mass, respectively, during these seasons. Isoprene  
568 derived organosulfate ( $m/z$  215, 2-methyltetrol derived), formed from isoprene derived  
569 epoxydiols (IEPOX) under low NO<sub>x</sub> conditions, was the most abundant identified organosulfate  
570 (up to 167 ng/m<sup>3</sup> in summer). This observation is consistent with observations of low NO<sub>x</sub>  
571 levels (< 1ppb on average) at our study site. Nighttime nitrate radical chemistry is most likely the  
572 dominant formation mechanism for nitrooxy-organosulfates measured at this remote site with  
573 background level NO<sub>x</sub>.

574 Nitro-aromatics were most abundant at our study site during the fall (up to 0.01% of OM  
575 mass). Moderate correlations were observed between nitro-aromatics and the biomass burning  
576 marker levoglucosan, indicating a common origin. Nitro-aromatics also correlated well with EC  
577 across seasons. Highest concentrations of nitro-aromatics, specifically nitrocatechol and methyl-  
578 nitrocatechol, were associated with aged biomass burning plumes as indicated by  
579 correspondingly high concentrations of terpenoic acids.

580 Bulk measurements determined that WSOC accounted for 62±13% of OC throughout the  
581 entire study period without significant seasonal variability. PMF analysis indicated that a  
582 significant portion of this organic carbon was associated with a resolved factor of WSON  
583 containing OM. As a component of total nitrogen in PM<sub>2.5</sub>, largest contributions of WSON to  
584 WSTN were observed in spring (~ 18% w/w) and lowest in the fall (~10% w/w). On average,  
585 identified nitro-aromatic and nitrooxy-organosulfate compounds accounted for a small fraction  
586 of WSON, ranging from ~ 1% in spring to ~ 4% in fall, though were observed to contribute as  
587 much as 28% w/w of WSON in individual samples. Of the organic N compounds speciated in  
588 this study, nitrooxy-organosulfates dominated over nitro-aromatics as a source of organic  
589 nitrogen, contributing > 90% to WSON across seasons. As a component of WSON, nitro-  
590 aromatics were most important during episodes of biomass burning, when their contribution to  
591 identified and total WSON was as much as 32% and 3%, respectively. Concentration weighted



592 average N/C ratios for compounds identified in this study were estimated to be 0.003. This  
593 number is an order of magnitude lower than the overall N/C ratio observed, indicating a  
594 predominance of other uncharacterized N species. Other N containing substituents of WSON  
595 could include amino acids, amines, urea and N-heterocyclic compounds as well as substances of  
596 biological origin such as spores, pollens and bacteria (Cape et al., 2011; Neff et al., 2002a).  
597 Ratios of WSON to WSOC indicate organic C being most enriched by organic N during spring,  
598 perhaps reflecting a spring maximum in seasonal emissions of organic N from biological sources  
599 combined with smaller contributions from secondary atmospheric processes (e.g., nitrooxy-  
600 organosulfates).

601 Although nitro-aromatics and nitrooxy-organosulfates contribute a relatively small  
602 fraction of organic N in PM<sub>2.5</sub> at our study site, our observations shed light on this complex but  
603 largely unknown portion of the atmospheric N budget. Our results provide further understanding  
604 of the patterns and composition of SOA in a remote mountain environment previously  
605 uncharacterized. Similar to our results, other studies generally find that individual groups of  
606 organic N compounds (e.g., amines, amino acids, urea) cannot explain the majority of bulk  
607 WSON, (Cape et al., 2011; Day et al., 2010; Place et al., 2017; Samy et al., 2013), which  
608 globally accounts for ~25% of total N in rainfall (Cape et al., 2011; Jickells et al., 2013). As  
609 methodological advances allow for greater speciation of this large pool of atmospheric N, future  
610 work should emphasize analysis of both primary and secondary forms of organic N in individual  
611 samples, in addition to bulk analyses, so that a more complete picture of organic N composition  
612 may be developed for specific atmospheric chemical and meteorological conditions.  
613 Additionally, as progress is made in better characterizing the composition and sources of  
614 atmospheric organic N, the ecological and atmospheric science communities must work together  
615 to develop a better understanding of the role of atmospheric organic N in ecosystem N cycling.

616

#### 617 **Supplemental Information available**

618

#### 619 **Acknowledgements**

620

621 We would like to acknowledge Pamela Barfield, Ryan Daly, Aleksandra Djurkovic, David  
622 Kirchgessner, John Offenberg, Bakul Patel and Bill Preston for laboratory and field support. We  
623 also would like to thank Joshua G. Hemann and Michael P. Hannigan for the PMF source codes



and Christopher Oishi, Patsy Clinton and Chuck Marshall for assistance with meteorological data sets. We would like to thank the U.S. Forest Service, Southern Research Station for the opportunity to conduct this study at the Coweeta Hydrologic Laboratory and for the contribution of meteorological data used in our analysis. We also thank internal EPA reviewers Chris Geron and Havala Pye for their comments and suggestions. The views expressed in this article are those of the authors and do not necessarily represent the views or policies of the U.S. EPA. Mention of trade names does not constitute endorsement or recommendation of a commercial product by U.S. EPA.

## References

- Altieri, K.E., Turpin, B.J., and Seitzinger S.P., 2009. Composition of dissolved organic nitrogen in continental precipitation investigated by Ultra-High Resolution FT-ICR Mass Spectrometry. *Environmental Science and Technology* 43, 6950-6955.
- Benedict, K.B., 2012. Observations of atmospheric reactive nitrogen species and nitrogen deposition in the Rocky Mountains. Dissertation, Colorado State University.  
<https://dspace.library.colostate.edu/handle/10217/71545>
- Birch, M. E. and Cary, R. A.: Elemental carbon-based method for monitoring occupational exposures to particulate diesel exhaust, *Aerosol Science and Technology*, 25, 221–241, 1996.
- Bobbink, R., Hornung M., and Roelofs, J.M., 1998. The effects of air-borne nitrogen pollutants on species diversity in natural and semi-natural European vegetation. *Journal of Ecology* 86, 717-738.
- Bolstad, P.V., Swank, W., Vose, J., 1998. Predicting Southern Appalachian overstory vegetation with digital terrain data. *Landscape Ecology* 13, 271-283.
- Bragazza, L., Freeman, C., Jones, T., Rydin, H., Limpens, J., Fenner, N., Ellis, T., Gerdol, R., Hajek, M., Iacumin, P., Kutnar, L., Tahvanainen, T., and Toberman, H., 2006. Atmospheric nitrogen deposition promotes carbon loss from peat bogs. *Proceedings of the national academy of Science* 103, 19386-19389.
- Budisulistiorini, S.H., Nenes, A., Carlton, A.G., Surratt, J.D., McNeill, V.F., Pye, H.O.T., 2017. Simulating aqueous-phase isoprene-epoxydiol(IEPOX) secondary organic aerosol production during the 2013 Southern Oxidation and Aerosol Study(SOAS). *Environmental Science and Technology* 51, 5026-5034.
- Cape, J.N., Cornell, S.E., Jickells, T.D., Nemitz, E., 2011. Organic nitrogen in the atmosphere- Where does it come from? A review of sources and methods. *Atmospheric Research* 102, 30-48.
- Chan, M.N., Surratt, J.D., Claeys, M., Edgerton, E.S., Tanner, R.L., Shaw, S.L., Zheng, M., Knipping, E.M., Eddingsaas, N.C., Wennberg, P.O., Seinfeld, J.H., 2010. Characterization and



- quantification of isoprene-derived epoxydiols in ambient aerosol in the Southeastern United States. *Environmental Science and Technology* 44, 4590-4596.
- Chen, Y., Bond, T.C., 2010. Light absorption by organic carbon from wood combustion. *Atmospheric Chemistry and Physics* 10, 1773-1787.
- Cheng, Y., He, K.-b., Du, Z.-y., Engling, G., Liu, J.-m., Ma, Y.-l., Zheng, M., Weber, R.J., 2016. The characteristics of brown carbon aerosol during winter in Beijing. *Atmospheric Environment* 127, 355-364.
- Claeys, M., Graham, B., Vas, G., Wang, W., Vermeylen, R., Pashynska, V., Cafmeyer, J., Guypn, P., Andreae, M.O., Artaxo, P., Maenhaut, W., 2004. Formation of secondary organic aerosols through photooxidation of isoprene. *Science* 303, 1173-1176.
- Claeys, M., Szmigielski, R., Kourtchev, I., Van Der Veken, P., Vermeylen, R., Maenhaut, W., Jaoui, M., Kleindienst, T.E., Lewandowski, M., Offenberg, J.H., Edney, E.O., 2007. Hydroxydicarboxylic acids: Markers for secondary organic aerosol from the photooxidation of  $\alpha$ -pinene. *Environmental Science and Technology* 41, 1628-1634.
- Claeys, M., Iinuma, Y., Szmigielski, R., Surratt, J.D., Blockhuys, F., Van Alsenoy, C., Boge, O., Sierau, B., Gomez-Gonzalez, Y., Vermeylen, R., Van Der Veken, P., Shahgholi, M., Chan, A.W.H., Herrmann, H., Seinfeld, J.H., Maenhaut, W., 2009. Terpenylic acid and related compounds from the oxidation of  $\alpha$ -pinene: Implications for new particle formation and growth above forests. *Environmental Science and Technology* 43, 6976-6982.
- Claeys, M.; Vermeylen, R.; Yasmeen, F.; Gómez-González, Y.; Chi, X. G.; Maenhaut, W.; Mészáros, T.; Salma, I., 2012. Chemical characterisation of humic-like substances from urban, rural and tropical biomass burning environments using liquid chromatography with UV/vis photodiode array detection and electrospray ionization mass spectrometry. *Environmental Chemistry* 9, 273-284.
- Darer, A.I., Cole-Filipiak, N.C., O'Connor, A.E., Elrod, M.J., 2011. Formation and stability of atmospherically relevant isoprene-derived organosulfates and organonitrates. *Environmental Science and Technology* 45, 1895-1902.
- Day, D. A., Liu, S., Russell, L. M. and Ziemann, P. J., 2010. Organonitrate group concentrations in submicron particles with high nitrate and organic fractions in coastal southern California. *Atmospheric Environment* 44, 1970-1979.
- Doney, S.C., Mahowald, N., Lima, I., Feely, R.A., Mackenzie, F.T., Lamarque, J-F., and Rasch, P.J., 2007. Impact of anthropogenic atmospheric nitrogen and sulfur deposition on ocean acidification and the inorganic carbon system. *Proceedings of the national academy of Science* 104, 14580-14585.
- Elbert, W., Taylor, P.E., Andreae, M.O., Poschl, U., 2007. Contribution of fungi to primary biogenic aerosols in the atmosphere: wet and dry discharged spores, carbohydrates, and





- 710 inorganic ions. *Atmospheric Chemistry and Physics* 7, 4569-4588.  
711  
712 Fehsenfeld, F.C., Dickerson, R.R., Hubler, G., Luke, W.T., Nunnermacker, L.J., Williams, E.J.,  
713 Roberts, J.M., Calvert, J.G., Curran, C.M., Delany, A.C., Eubank, C.S., Fahey, D.W., Fried, A.,  
714 Grandrud, B.W., Langford, A.O., Murphy, P.C., Norton, R.B., Pickering, K.E., Ridley, B.A., 1987.  
715 A ground-based intercomparison of NO, NO<sub>x</sub> and NO<sub>y</sub> measurement techniques. *Journal of*  
716 *Geophysical Research* 92, 14710-14722.  
717  
718 Gaston, C.J., Lopez-Hifiker, F.D., Whybrew, L.E., Hadley, O., McNair, F., Gao, H., Jaffe, D.A.,  
719 Thornton, J.A., 2016. Online molecular characterization of fine particulate matter in Port Angeles,  
720 WA: Evidence for a major impact from residential wood smoke. *Atmospheric Environment* 138,  
721 99-107.  
722  
723 Gomez-Gonzalez, Y., Surratt, J. D., Cuyckens, F., Szmigielski, R., Vermeulen, R., Jaoui, M.,  
724 Lewandowski, M., Offenberg, J. H., Kleindienst, T. E., Edney, E. O., Blockhuys, F., Van  
725 Alsenoy, C., Maenhaut, W., and Claeys, M., 2008. Characterization of organosulfates from the  
726 photooxidation of isoprene and unsaturated fatty acids in ambient aerosol using liquid  
727 chromatography/(-) electrospray ionization mass spectrometry, *Journal of Mass Spectrometry*,  
728 43, 371-382.  
729  
730 Gomez-Gonzalez, Y., Wang, W., Vermeulen, R., Chi, X., Neirynck, J., Janssens, I.A., Maenhaut,  
731 W., Claeys, M., 2012. Chemical characterization of atmospheric aerosols during a 2007 summer  
732 field campaign at Brasschaat, Belgium: sources and source processes of biogenic secondary  
733 organic aerosol. *Atmospheric Chemistry and Physics* 12, 125-138.  
734  
735 Gonzalez Benitez, J.M., Cape, J.N., Heal, M.R., van Dijk, N., Vidal Diez, A., 2009. Atmospheric  
736 nitrogen deposition in south-east Scotland: Quantification of the organic nitrogen fraction in wet,  
737 dry and bulk deposition. *Atmospheric Environment* 43, 4087-4094.  
738  
739 Hamilton, J.F., Alfara, M.R., Robinson, N., Ward, M.W., Lewis, A.C., McFiggans, G.B., Coe,  
740 H., Allan, D., 2013. Linking biogenic hydrocarbons to biogenic aerosol in the Borneo rainforest.  
741 *Atmospheric Chemistry and Physics* 13, 11295-11305.  
742  
743 He, Q-F., Ding, X., Wang, X-M., Yu, J.Z., Fu, X-X., Liu, T-Y., Zhang, Z., Xue, J., Chen, D-H.,  
744 Zhong, L-J., Donadue, N.M., 2014. Organosulfates from pinene and isoprene over the Pearl  
745 River Delta, South China: Seasonal variation and implication in formation mechanisms.  
746 *Environmental Science and Technology* 48, 9236-9245.  
747  
748 Hecobian, A., Zhang, X., Zheng, M., Frank, N., Edgerton, E.S., Weber, R.J., 2010. Water  
749 Soluble Organic Aerosol material and the light-absorption characteristics of aqueous extracts  
750 measured over the Southeastern United States. *Atmospheric Chemistry and Physics* 10, 5965-  
751 5977.  
752  
753 Hemann, J.G., Brinkman, G.L., Dutton, S.J., Hannigan, M.P., Milford, J.B., Miller, S.L., 2009.  
754 Assessing positive matrix factorization model fit: a new method to estimate uncertainty and bias  
755 in factor contributions at the measurement time scale. *Atmospheric Chemistry and Physics* 9,  
756 497-513.



- 757  
758 Hungate, B.A., Dukes, J.S., Shaw, M.R., Luo, Y., and Field C.B., 2003. Nitrogen and Climate  
759 Change. *Science* 302, 1512-1513.  
760  
761 Iinuma, Y., Boge, O., Kahnt, A., Herrmann, H., 2009. Laboratory chamber studies on the  
762 formation of organosulfates from reactive uptake of monoterpene oxides. *Physical Chemistry*  
763 *Chemical Physics* 11, 7985-7997.  
764  
765 Iinuma, Y., Boge, O., Grafe, R., Herrmann, H., 2010. Methyl-nitrocatechols : atmospheric tracers  
766 compounds for biomass burning secondary organic aerosols. *Environmental Science and*  
767 *Technology* 44, 8453-8459.  
768  
769 Iinuma, Y., Keywood, M., Herrmann, H., 2016. Characterization of primary and secondary  
770 organic aerosols in Melbourne airshed: The influence of biogenic emissions, wood smoke and  
771 bushfires. *Atmospheric Environment* 130, 54-63.  
772  
773 Jickells, T., Baker, A.R., Cape, J.N., Cornell, S.E., Nemitz, E., 2013. The cycling of organic  
774 nitrogen through the atmosphere. *Philosophical Transactions of the Royal Society B*  
775 368:20130115.  
776  
777 Kahnt, A., Behrouzi, S., Vermeylen, R., Safi Shalamzari, M., Vercauteren, J., Roekens, E.,  
778 Claeys, M., Maenhaut, W., 2013. One-year study of nitro-organic compounds and their relation  
779 to wood burning in PM10 aerosol from a rural site in Belgium. *Atmospheric Environment* 81,  
780 561-568.  
781  
782 Kahnt, A., Iinuma, Y., Blockhuys, F., Mutzel, A., Vermeylen, R., Kleindienst, T.E., Jaoui, M.,  
783 Offenberg, J.H., Lewandowski, M., Boge, O., Herrmann, H., Maenhaut, W., Claeys, M., 2014.  
784 2-Hydroxyterpenylic acid: an oxygenated marker compound for  $\alpha$ -pinene secondary organic  
785 aerosol in ambient fine aerosol. *Environmental Science and Technology* 48, 4901-4908.  
786  
787 Keene, W.C., Montag, J.A., Maben, J.R., Southwell, M., Leonard, J., Church, T.M., Moody, J.L.,  
788 Galloway, J.N., 2002. Organic nitrogen in precipitation over Eastern North America.  
789 *Atmospheric Environment* 36, 4529-4540.  
790  
791 Kitanovski, Z., Grgic, I., Vermeylen, R., Claeys, M., Maenhaut, W., 2012. Liquid  
792 chromatography tandem mass spectrometry method for characterization of monoaromatic nitro-  
793 compounds in atmospheric particulate matter. *Journal of Chromatography A* 1268, 35-43.  
794  
795 Kleindienst, T. E., Jaoui, M., Lewandowski, M., Offenberg, J.H., Lewis, C.W., Bhawe, P.V.,  
796 Edney, E.O., 2007. Estimates of the contributions of biogenic and anthropogenic hydrocarbons  
797 to secondary organic aerosol at a southeastern US location. *Atmospheric Environment* 41, 8288-  
798 8300.  
799  
800 Lin, M., Walker, J., Geron, C., Khlystov, A., 2010. Organic nitrogen in PM2.5 aerosol at a forest  
801 site in the Southeast US. *Atmospheric Chemistry and Physics* 10, 2145-2157.  
802



- 803 Lin, Y.-H., Zhang, H., Pye, H.O.T., Zhang, Z., Marth, W.J., Park, S., Arashiro, M., Cui, T.,  
804 Hapsari Budisulistiorini, S., Sexton, K.G., Vizuete, W., Xie, Y., Luecken, D.J., Piletic, I.R.,  
805 Edney, E.O., Bartolotti, L.J., Gold, A., Surratt, J.D., 2013a. Epoxide as a precursor to secondary  
806 organic aerosol formation from isoprene photooxidation in the presence of nitrogen oxides.  
807 *Proceedings of the National Academy of Science* 110, 6718-6723.
- 808
- 809 Lin, Y.-H., Knipping, E.M., Edgerton, E.S., Shaw, S.L., Surratt, J.D., 2013b. Investigating the  
810 influences of SO<sub>2</sub> and NH<sub>3</sub> levels on isoprene-derived secondary organic aerosol formation  
811 using conditional sampling approaches. *Atmospheric Chemistry and Physics* 13, 8457-8470.
- 812
- 813 Liu, J., Bergin, M., Guo, H., King, L., Kotra, N., Edgerton, E., Weber, R.J., 2013. Size-resolved  
814 measurements of brown carbon in water and methanol extracts and estimates of their  
815 contribution to ambient fine-particle light absorption. *Atmospheric Chemistry and Physics* 13,  
816 12389-12404.
- 817
- 818 Liu, J., Scheuer, E., Dibb, J., Diskin, G.S., Ziemba, L.D., Thornhill, K.I., Anderson, B.E.,  
819 Wisthaler, A., Mikoviny, T., Devi, J.J., Bergin, M., Perring, A.E., Markovic, M.Z., Scheartz,  
820 J.P., Campuzano-Jost, P., Day, D.A., Jimenez, J.L., Weber, R.J., 2015. Brown carbon aerosol in  
821 the North American continental troposphere: sources, abundance, and radiative forcing.  
822 *Atmospheric Chemistry and Physics* 15, 7841-7858.
- 823
- 824 Lohse, K.A., Hope, D., Sponseller, R., Allen, J.O., Grimm, N.B., 2008. Atmospheric deposition  
825 of carbon and nutrients across an arid metropolitan area. *Science of the Total Environment* 402,  
826 95-105.
- 827
- 828 Magnani, F., Mencuccini, M., Borghetti, M., Berbigier, P., Berninger, F., Delzon, S., Grelle, A.,  
829 Hari, P., Jarvis, P.G., Kolari, P., Kowalski, A.S., Lankreijer, H., Law, B.E., Lindroth, A.,  
830 Loustau, D., Manca, G., Moncrieff, J.B., Rayment, M., Tedeschi, V., Valentini, R., Grace, J.,  
831 2007. The human footprint in the carbon cycle of temperate and boreal forests. *Nature* 447, 848-  
832 850.
- 833
- 834 Meade, L.E., Riva, M., Blomberg, M.Z., Brock, A.K., Qualters, E.M., Siejack, R.A.,  
835 Ramakrishnan, K., Surratt, J.D., Kautzman, K.E., 2016. Seasonal variation of fine particulate  
836 organosulfates derived from biogenic and anthropogenic hydrocarbons in the mid-Atlantic  
837 United States. *Atmospheric Environment* 145, 405-414.
- 838
- 839 Miniati, C.F., Laseter, S.H., Swank, W.T., Swift, L.W. Jr., 2015. Daily air temperature, relative  
840 humidity, vapor pressure, PPFD, wind speed and direction for climate stations at the Coweeta  
841 Hydrologic Lab, North Carolina. Fort Collins, CO: Forest Service Research Data Archive.  
842 Updated 28 February 2017. <https://doi.org/10.2737/RDS-2015-0042>
- 843
- 844
- 845 Miyazaki, Y., Fu, P., Ono, K., Tachibana, E., Kawamura, K., 2014. Seasonal cycles of water-  
846 soluble organic nitrogen aerosols in a deciduous broadleaf forest in northern Japan. *Journal of*  
847 *Geophysical Research: Atmospheres* 119, 1440-1454.
- 848



- 849 Mohr, C., Lopez-Hilfiker, F.D., Zotter, P., Prevot, A.S.H., Xu, L., Ng, N.L., Herndon, S.C.,  
850 Williams, L.R., Franklin, J.P., Zahniser, M.S., Worsnop, D.R., Knighton, W.B., Aiken, A.C.,  
851 Gorkowski, K.J., Dubey, M.K., Allan, J.D., Thornton, J.A., 2013. Contribution of nitrated  
852 phenols to wood burning brown carbon light absorption in Detling, United Kingdom during  
853 winter time. *Environmental Science and Technology* 47, 6316-6324.  
854
- 855 Muller, L.; Reinnig, M.-C.; Naumann, K. H.; Saathoff, H.; Mentel, T. F.; Donahue, N. M.;  
856 Hoffmann, T., 2012. Formation of 3-methyl-1,2,3- butanetricarboxylic acid via gas phase  
857 oxidation of pinonic acid – a mass spectrometric study of SOA aging. *Atmospheric Chemistry*  
858 *and Physics* 12, 1483–1496.  
859
- 860 Neff, J.C., Holland, E.A., Dentener, F.J., McDowell, W.H., Russell, K.M., 2002a. The origin,  
861 composition and rates of organic nitrogen depiction: A missing piece of the nitrogen cycle?  
862 *Biogeochemistry* 57/58, 99-136.  
863
- 864 Neff, J.C., Townsend, A.R., Gleixner, G., Lehman, S.J., Turnbull, J., Bowman, W., 2002b.  
865 Variable effects of nitrogen additions on the stability and turnover of soil carbon. *Nature* 419,  
866 915-917.  
867
- 868 Oishi, A.C., Miniati, C.F., Novick, K.A., Brantley, S.T., Vose, J.M., Walker, J.T., 2017. Warmer  
869 temperatures reduce net carbon uptake, but do not affect water use, in a mature southern  
870 Appalachian forest. *Agricultural and Forest Meteorology*. In press.  
871
- 872 Ollinger, S.V., Aber, J.D., Reich, P.B., Freuder, R.J., 2002. Interactive effects of nitrogen  
873 deposition, tropospheric ozone, elevated CO<sub>2</sub> and land use history on the carbon dynamics of  
874 northern hardwood forests. *Global Change Biology* 8, 545-562.  
875
- 876 Paatero, P. User's Guide for Positive Matrix Factorization Program PMF2 and PMF3, Part 1:  
877 Tutorial. University of Helsinki: Helsinki, Finland, 1998a.  
878
- 879 Paatero, P. User's Guide for Positive Matrix Factorization Program PMF2 and PMF3, Part 2:  
880 Reference. University of Helsinki: Helsinki, Finland, 1998b.  
881
- 882 Place, B. K., Quilty, A. T., Di Lorenzo, R. A., Ziegler, S. E., and VandenBoer, T. C. ,2017.  
883 Quantitation of 11 alkylamines in atmospheric samples: separating structural isomers by ion  
884 chromatography, *Atmospheric Measurement Techniques* 10, 1061–1078.  
885
- 886 Pregitzer, K.S., Burton, A.J., Zak, D.R., and Talhelm, A.F., 2008. Simulated chronic nitrogen  
887 deposition increases carbon storage in Northern Temperate forests. *Global Change Biology* 14,  
888 142-153.  
889
- 890 Samy, S., Robinson, J., Rumsey, I.C., Walker, J.T., Hays, M.D., 2013. Speciation and trends of  
891 organic nitrogen in southeastern U.S. fine particulate matter (PM<sub>2.5</sub>). *Journal of Geophysical*  
892 *Research: Atmospheres* 118, 1996-2006.  
893
- 894 Shalamzari, M.S., Vermeylen, R., Blockhuys, F., Kleindienst, T.E., Lewandowski, M.,  
895 Szmigielski, R., Rudzinski, K.J., Spolnik, G., Danikiewicz, W., Maenhaut, W., Claeys, M., 2016.



- 896 Characterization of polar organosulfates in secondary organic aerosol from the unsaturated  
897 aldehydes 2-E-pentenal, 2-E-hexenal, and 3-Z-hexenal. *Atmospheric Chemistry and Physics* 16,  
898 7135-7148.  
899
- 900 Simkin, S.M., Allen, E.B., Bowman, W.D., Clark, C.M., Belnap, J., Brooks, M.L., Cade, B.S.,  
901 Collins, S.L., Geiser, L.H., Gilliam, F.S., Jovan, S.E., Pardo, L.H., Schulz, B.K., Stevens, C.J.,  
902 Suding, K.N., Throop, H.L., and Waller, D.M., 2016. Conditional vulnerability of plant diversity  
903 to atmospheric nitrogen deposition across the United States. *Proceedings of the national*  
904 *academy of Science* 113, 4086-4091.  
905
- 906 Surratt, J. D., Murphy, S.M., Kroll, J.H., Ng, N.L., Hildebrandt, L., Sorooshian, A., Szmigielski,  
907 R., Vermeylen, R., Maenhaut, W., Claeys, M., Flagen, R.C., Seinfeld, J.H., 2006. Chemical  
908 composition of secondary organic aerosol formed from the photooxidation of isoprene. *Journal*  
909 *of Physical Chemistry A* 110, 9665-9690.  
910
- 911 Surratt, J.D., Kroll, J.H., Kleindienst, T.E., Edney, E.O., Claeys, M., Sorooshian, A., Ng, N.L.,  
912 Offenberg, J.H., Lewandowski, M., Jaoui, M., Flagan, R.C., Seinfeld, J.H., 2007. Evidence for  
913 organosulfates in secondary organic aerosol. *Environmental Science and Technology* 41, 517-  
914 527.  
915
- 916 Surratt, J.D., Gomez-Gonzalez, Y., Chan, A.W.H., Vermeylen, R., Shahgholi, M., Kleindienst,  
917 T.E., Edney, E.O., Offenberg, J.H., Lewandowski, M., Jaoui, M., Maenhaut, W., Claeys, M.,  
918 Flagan, R.C., Seinfeld, J.H., 2008. Organosulfate formation in biogenic organic aerosol. *Journal*  
919 *of physical chemistry A* 112, 8345-8378.  
920
- 921 Surratt, J.D., Chan, A.W.H., Eddingsaas, N.C., Chan, M.N., Loza, C.L., Kwan, A.J., Hersey,  
922 S.P., Flagan, R.C., Wennberg, P.O., Seinfeld, J.H., 2010. Reactive intermediates revealed in  
923 secondary organic aerosol formation from isoprene. *Proceedings of the National Academy of*  
924 *Science* 107, 6640-6645.  
925
- 926 Swank, W.T. and D.A. Crossley, Jr..1988. Introduction and site description. In *Forest Hydrology*  
927 *and Ecology at Coweeta*. 169 pp. Edited by W.T. Swank and D.A. Crossley, Jr. Springer-Verlag,  
928 Berlin.  
929
- 930 Swift, L.W..Jr., G.B. Cunningham and J.E. Douglass. 1988. *Climatology and Hydrology*. In  
931 *Forest Hydrology and Ecology at Coweeta*. 469 pp. Edited by W.T. Swank and D.A. Crossley.  
932 Jr. Springer-Verlag. Berlin  
933
- 934 Szmigielski, R.; Surratt, J. D.; Gómez-González, Y.; Van der Veken, P.; Kourtchev, I.;  
935 Vermeylen, R.; Blockhuys, F.; Jaoui, M.; Kleindienst, T. E.; Lewandowski, M.; Offenberg, J. H.;  
936 Edney, E. O.; Seinfeld, J. H.; Maenhaut, W.; Claeys, M., 2007. 3-methyl-1,2,3-  
937 butanetricarboxylic acid: An atmospheric tracer for terpene secondary organic aerosol.  
938 *Geophysical Research Letter* 34, L24811.  
939



- 940 U.S. EPA, 2017. U.S. Environmental Protection Agency Clean Air Markets Division,  
941 Clean Air Status and Trends Network (CASTNET). Hourly ozone and meteorology.  
942 Available at [www.epa.gov/castnet](http://www.epa.gov/castnet). Date accessed: 01/15/2017.  
943
- 944 Walker, J.T., Dombek, T.L., Green, L.A., Gartman, N., Lehmann, C.M.B., 2012. Stability of  
945 organic nitrogen in NADP wet deposition samples. *Atmospheric Environment* 60, 573-582.  
946
- 947 Williams, E.J.; Baumann, K.; Roberts, J.M.; Bertman, S.B.; Norton, R.B.; Fehsenfeld, F.C.;  
948 Springston, S.R.; Nunnermacker, L.G.; Newman, L.; Olszyna, K.; Meagher, J.; Hartsell, B.;  
949 Edgerton, E.; Perason, J.R.; Rodgers, M.O., 1998. Intercomparison of ground-based NO<sub>y</sub>  
950 measurements techniques. *Journal of Geophysical Research: Atmospheres* 103, 22261-22280.  
951
- 952 Worton, D. R., Goldstein, A. H., Farmer, D. K., Docherty, K. S., Jimenez, J. L., Gilman, J. B.,  
953 Kuster, W. C., de Gouw, J., Williams, B. J., Kreisberg, N. M., Hering, S. V., Bench, G., McKay,  
954 M., Kristensen, K., Glasius, M., Surratt, J. D., Seinfeld, J. H., 2011. Origins and composition of  
955 fine atmospheric carbonaceous aerosol in the Sierra Nevada Mountains, California. *Atmospheric  
956 Chemistry and Physics* 11, 10219-10241.  
957
- 958 Worton, D.R., Surratt, J.D., LaFranchi, B.W., Chan, A.W.H., Zhao, Y., Weber, R.J., Park, J-H.,  
959 Gilman, J.B., de Gouw, J., Park, C., Schade, G., Beaver, M., St. Clair, J.M., Crounse, J.,  
960 Wennberg, P., Wolfe, G.M., Harrold, S., Thornton, J.A., Farmer, D.K., Docherty, K.S., Cubison,  
961 M.J.M., Jimenez, J-L., Frossard, A.A., Russell, L.M., Kristensen, K., Glasius, M., Mao, J., Ren,  
962 X., Brune, W., Browne, E.C., Pusede, S.E., Cohen, R.C., Seinfeld, J.H., Goldstein, A.H., 2013.  
963 Observational insights into aerosol formation from isoprene. *Environmental Science and  
964 Technology* 47, 11403-11413.  
965
- 966 Xie, M., Hannigan, M.P., Dutton, S.J., Milford, J.B., Hemann, J.G., Miller, S.L., Schauer, J.J.,  
967 Peel, J.L., Vedal, S., 2012. Positive matrix factorization of PM<sub>2.5</sub>: Comparison and implications  
968 of using different speciation data sets. *Environmental Science & Technology* 46, 11962-11970  
969
- 970 Xie, M., Barsanti, K.C., Hannigan, M.P., Dutton, S.J., Vedal, S., 2013. Positive matrix  
971 factorization of PM<sub>2.5</sub> - eliminating the effects of gas/particle partitioning of semivolatile  
972 organic compounds. *Atmospheric Chemistry and Physics* 13, 7381-7393.  
973
- 974 Xie, M., Hannigan, M.P., Barsanti, K.C., 2014. Impact of Gas/Particle Partitioning of  
975 Semivolatile Organic Compounds on Source Apportionment with Positive Matrix Factorization.  
976 *Environmental Science & Technology* 48, 9053-9060.  
977
- 978 Zellweger, C., Ammann, M., Buchmann, B., Hofer, P., Lugauer, M., Ruttimann, R., Streit, N.,  
979 Weingartner, E., Baltensperger, U., 2000. Summertime NO<sub>y</sub> speciation at the Jungfrauoch,  
980 3580m above sea level, Switzerland. *Journal of Geophysical Research* 105, 6655-6667.  
981
- 982 Zhang, Y., Song, L., Liu, X.J., Li, W.Q., Lu, S.H., Zheng, L.X., Bai, Z.C., Cai, G.Y., Zhang,  
983 F.S., 2012. Atmospheric organic nitrogen deposition in China. *Atmospheric Environment* 46,  
984 195-204.



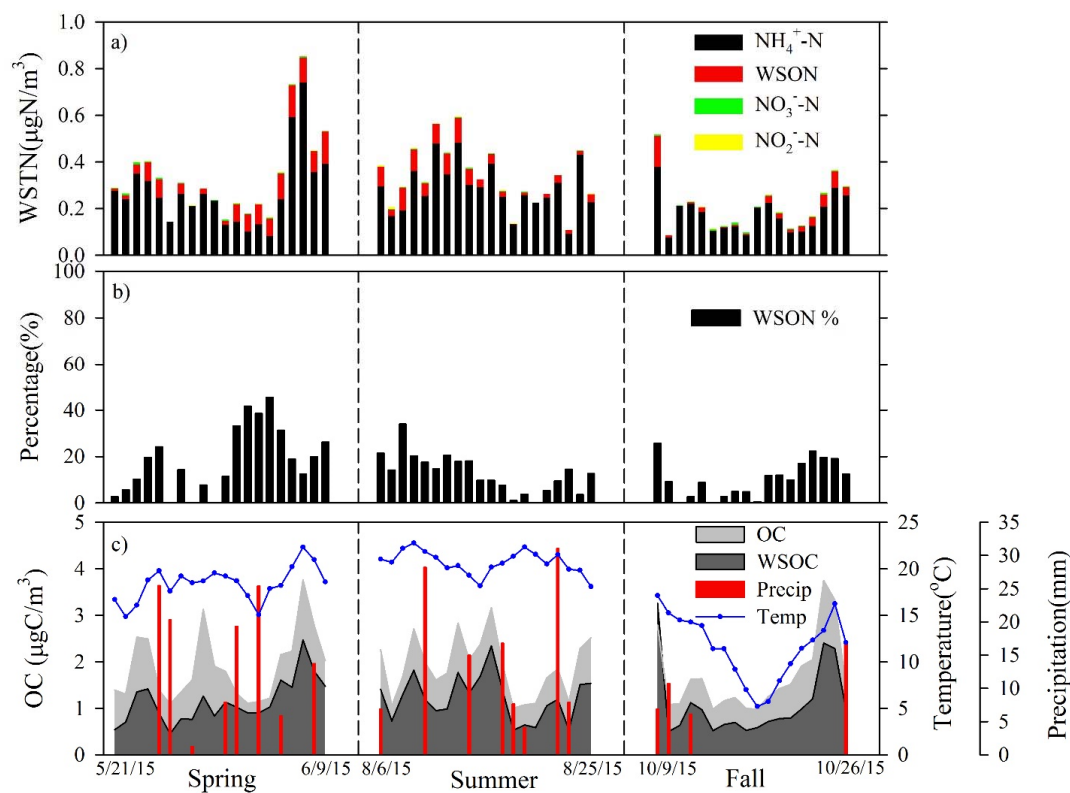


Figure 1. a) Individual concentrations of nitrogen components to WSTN ( $\text{NH}_4^+$ ,  $\text{NO}_3^-$ ,  $\text{NO}_2^-$  and WSON); b) Percent contribution of WSON to WSTN; c) Time series of OC, WSOC, temperature and precipitation. Start and end dates of each intensive sampling periods are shown.



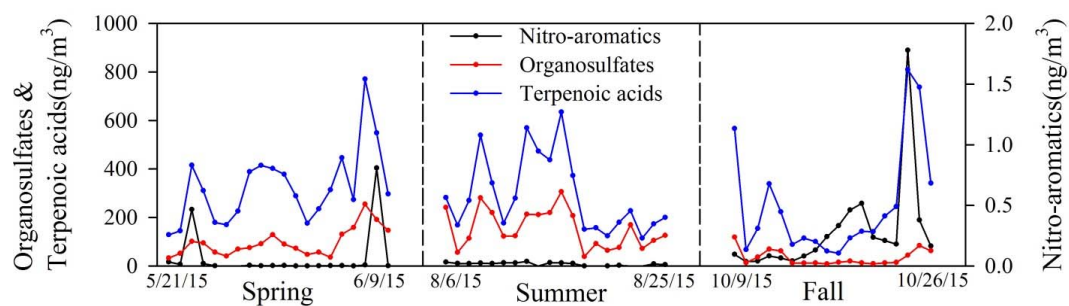


Figure 2. Time series of summed compound group concentrations of nitro-aromatics, organosulfates and terpenoic acids.

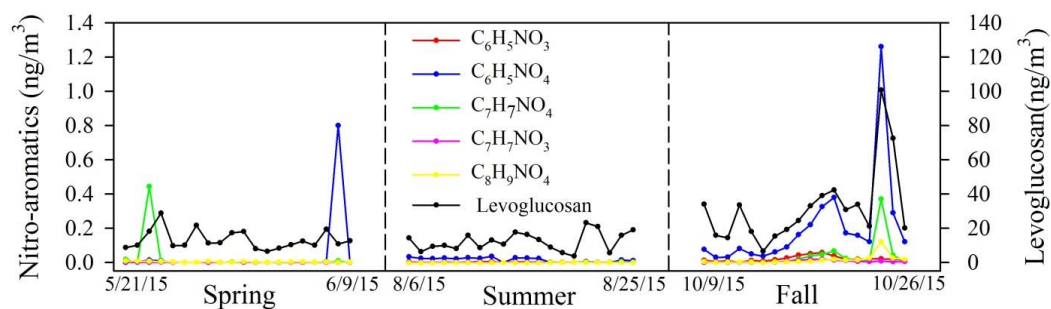


Figure 3. Time series of individual nitro-aromatics compounds as well as levoglucosan.

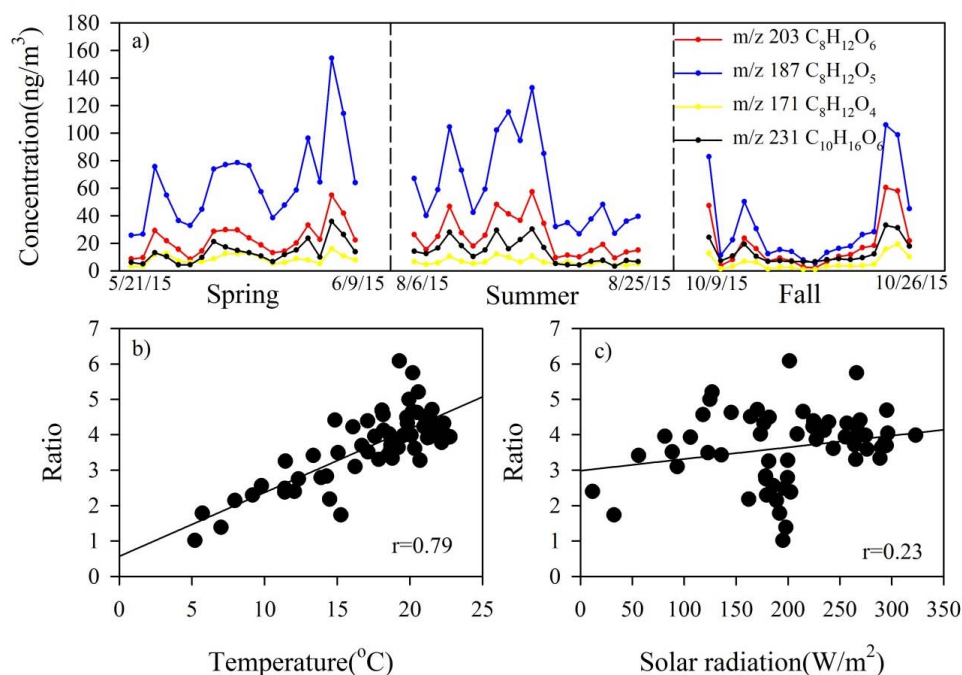


Figure 4. a) Time series of these four identified terpenoic acids(3-methyl-1,2,3-butanetricarboxylic acid(MBTCA, C<sub>8</sub>H<sub>12</sub>O<sub>6</sub>, m/z 203), 2-hydroxyterpenylic acid(C<sub>8</sub>H<sub>12</sub>O<sub>5</sub>, m/z 187), terpenylic acid(C<sub>8</sub>H<sub>12</sub>O<sub>4</sub>, m/z 171) and Diaterpenylic acid acetate(DTAA, C<sub>10</sub>H<sub>16</sub>O<sub>6</sub>,m/z 231)); b) correlation of concentration ratios of higher generation oxidation products( C<sub>8</sub>H<sub>12</sub>O<sub>6</sub>, m/z 203 and C<sub>8</sub>H<sub>12</sub>O<sub>5</sub>, m/z 187) to early oxidation fresh SOA products(C<sub>8</sub>H<sub>12</sub>O<sub>4</sub>, m/z 171 and C<sub>10</sub>H<sub>16</sub>O<sub>6</sub>,m/z 231) with temperature and ; c) with solar radiation.

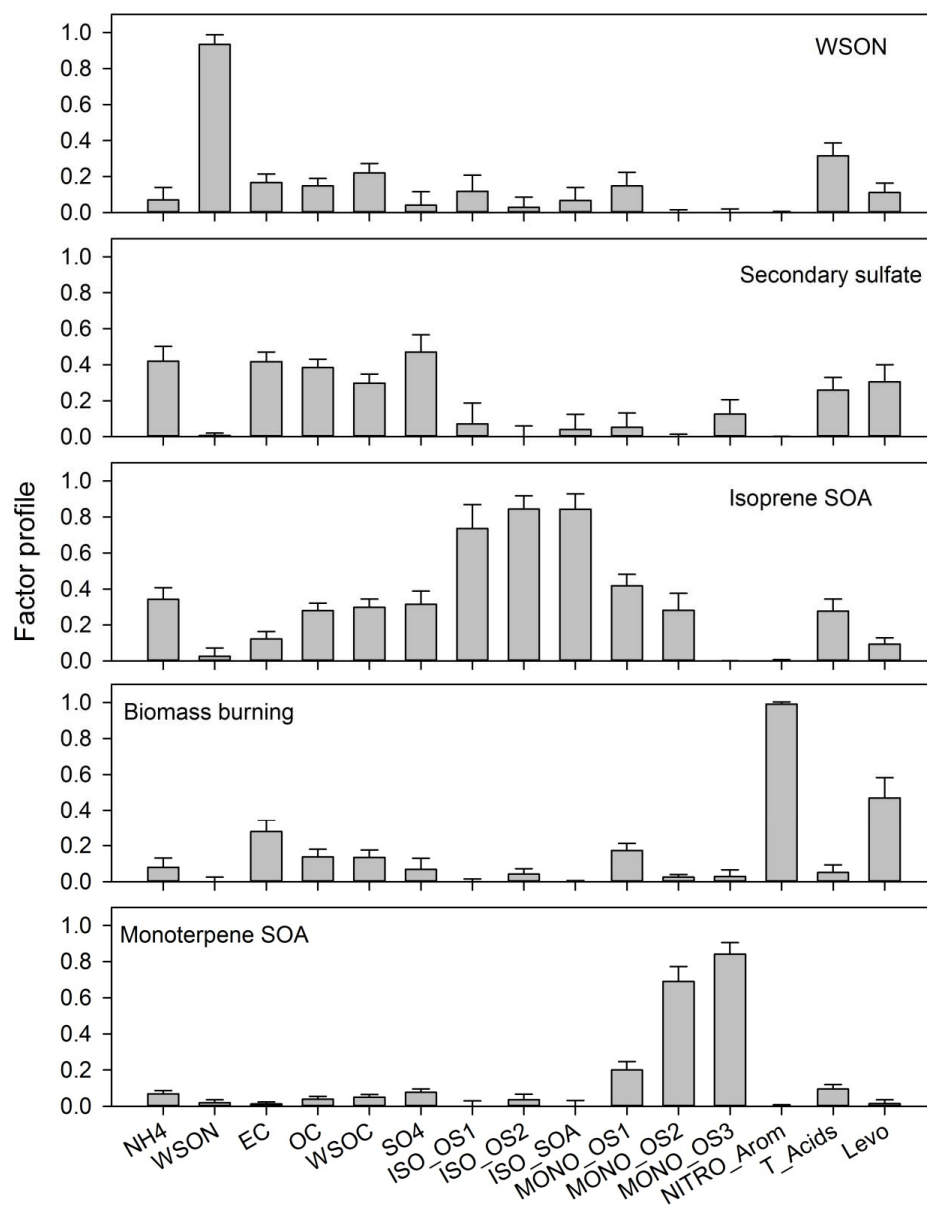


Figure 5. Normalized factor profiles (error bar represents one standard deviation).

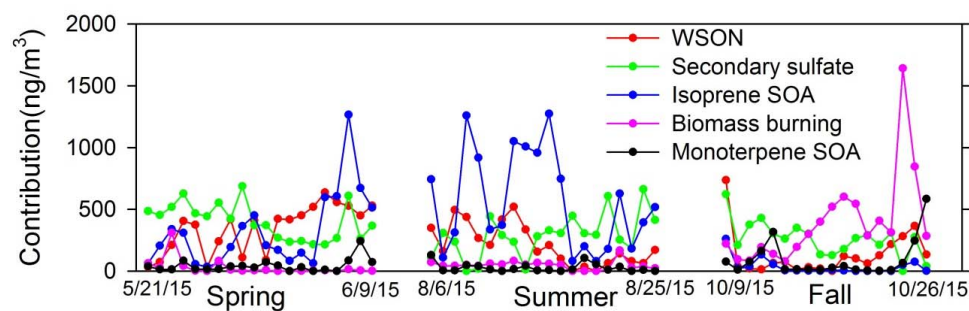


Figure 6. Time series of factor contributions to WSOC.



Table 1. Summary of particulate and gaseous species measured at Coweeta sampling site in 2015.

	Spring				Summer				Fall			
	mean	median	min	max	mean	median	min	max	mean	median	min	max
( $\mu\text{g}/\text{m}^3$ )												
OM ( $\text{OC}^*2$ )	3.77	3.41	2.18	7.52	3.80	3.79	2.00	6.32	3.36	2.85	1.96	7.49
EC	0.05	0.05	0.03	0.10	0.05	0.05	0.02	0.08	0.07	0.07	0.03	3.75
WSOC	1.14	1.03	0.45	2.47	1.22	1.24	0.53	2.34	1.09	0.78	0.50	3.25
WSTN	0.33	0.29	0.14	0.86	0.34	0.32	0.11	0.59	0.21	0.20	0.08	0.52
WSON	0.06	0.07	ND	0.14	0.05	0.03	ND	0.11	0.03	0.02	ND	0.13
$\text{NH}_4^+ - \text{N}$	0.27	0.24	0.08	0.74	0.29	0.28	0.09	0.48	0.18	0.17	0.08	0.38
$\text{NO}_3^- - \text{N}$	0.00	0.00	ND	0.01	0.00	0.00	ND	0.01	0.00	0.00	ND	0.01
$\text{NO}_2^- - \text{N}$	0.00	0.00	ND	0.00	0.00	0.00	ND	0.01	0.00	0.00	ND	0.00
$\text{SO}_4^{2-}$	0.99	0.93	0.26	2.44	1.01	0.95	0.31	1.85	0.63	0.58	0.30	1.33
$\text{O}_3$ (ppb)	25.1	21.6	13.9	46.1	15.8	15.8	9.0	22.8	19.4	20.5	11.1	26.9
$\text{NOx}$ (ppb)	0.75	0.79	0.45	1.03	0.54	0.58	0.24	0.91	0.65	0.68	0.43	0.89
Temp( $^{\circ}\text{C}$ )	18.4	18.6	14.8	22.3	20.7	20.6	18.1	22.8	11.6	11.7	5.2	17.1
RH%	81.7	84.9	61.0	94.8	82.1	83.1	71.9	88.5	77.7	74.9	65.1	92.0
Radiation	235	265	81	296	205	201	106	323	151	180	12	203

[illegible]



[illegible]



Table 3. Seasonal statistics of measured groups of compounds.

(ng/m <sup>3</sup> )	Spring				Summer				Fall			
	mean	median	min	max	mean	median	min	max	mean	median	min	max
Nitro- aromatics	0.07	0.00	ND	0.81	0.02	0.02	ND	0.04	0.28	0.17	0.04	1.78
Organo- sulfates <sup>1</sup>	96.77	83.05	33.07	255.17	153.36	125.41	38.93	306.66	34.69	15.27	0.17	118.68
Terpenoic acids	325.62	304.05	128.68	771.16	294.01	249.19	115.08	634.99	250.66	148.91	52.94	809.46
% of OM <sup>2</sup>												
%Nitro- aromatics	0.00	0.00	ND	0.02	0.00	0.00	ND	0.00	0.01	0.01	0.00	0.02
%Organo- sulfates	2.47	2.42	1.19	3.64	3.87	3.80	1.95	5.56	0.98	0.63	0.31	2.21
% Terpenoic acids	8.65	8.29	4.62	12.88	7.50	7.77	3.80	11.64	6.48	5.21	2.70	12.00

<sup>1</sup> including nitrooxy-organosulfates; <sup>2</sup> Fraction of each group of identified compounds (combined total) to organic matter

Table 4. Ratios of identified nitrogen containing compounds (nitroxy-organosulfates) to WSON.

(ngN/m <sup>3</sup> )	Spring				Summer				Fall			
	mean	median	min	max	mean	median	min	max	mean	median	min	max
WSON	59	74	ND	140	46	33	ND	105	25	15	ND	133
Identified ON	0.48	0.36	0.1	1.75	0.65	0.53	0.12	1.83	0.46	0.26	0.07	1.70
Identified ON/WSON %	1.02	0.64	ND	3.09	2.04	1.71	ND	7.84	4.37	1.50	ND	27.90